Coherent Nonlinear Optical Response of Graphene

E. Hendry,* P. J. Hale, J. Moger, and A. K. Savchenko
School of Physics, University of Exeter, EX4 4QL, United Kingdom

S. A. Mikhailov
Institute of Physics, University of Augsburg, D-86135 Augsburg, Germany

(Received 19 May 2010; published 26 August 2010)

We investigate the nonlinear optical properties of graphene flakes using four-wave mixing. The corresponding third-order optical susceptibility is found to be remarkably large and only weakly dependent on the wavelength in the near-infrared frequency range. The magnitude of the response is in good agreement with our calculations based on the nonlinear quantum response theory.

DOI: 10.1103/PhysRevLett.105.097401 PACS numbers: 78.67.Wj, 42.65.Ky, 78.47.nj

Graphene, a single sheet of carbon atoms in a hexagonal lattice, is the basic building block for all graphitic materials. Although it has been known as a theoretical concept for some time [1], a layer of graphene has only recently been isolated from bulk graphite and deposited on a dielectric substrate [2]. The great interest in studying graphene is driven by its linear, massless band structure

$$E_{\pm}(\mathbf{p}) = \pm V|\mathbf{p}| \tag{1}$$

and many unusual electrical, thermal, mechanical, and optical properties [3,4] [here the upper (lower) sign corresponds to the electron (hole) band, $\mathbf{p}$ is the quasimomentum, and $V \approx 10^6$ m/s is the Fermi velocity]. For example, the optical absorption of graphene has been shown to be wavelength independent ($\simeq$2.3% per layer) in a broad range of optical frequencies [5–7]. Recently, it has been predicted that the linear dispersion described by Eq. (1) should lead to strongly nonlinear optical behavior at microwave and terahertz frequencies [8]. At higher, optical frequencies one can also expect an enhanced optical nonlinearity as, due to graphene's band structure, interband optical transitions occur at all photon energies.

Here we report on the first observation of the coherent nonlinear optical response of graphene at visible and near-infrared frequencies. We show that graphene has an exceptionally high nonlinear response, described by the effective nonlinear susceptibility $|\chi^{(3)}| \sim 10^{-7}$ esu (electrostatic units). This nonlinearity is shown to be essentially dispersionless over the wavelength range in our experiments (emission at $\lambda_e \simeq 760$–840 nm). These results are in good agreement with predictions derived from nonlinear quantum response theory. The large optical nonlinearity of graphene can be used for exceptionally high-contrast imaging of single and multilayered graphene flakes.

Single- and few-layer graphene samples are fabricated using the method of mechanical exfoliation [2] and deposited onto a 100 μm thick glass cover slip. Prior to investigation in the nonlinear microscope, the layer thickness is estimated via contrast measurements under an optical microscope, using a method similar to Ref. [9]. To investigate the nonlinear response of graphene flakes, we employ the four-wave mixing technique [10]. This involves the generation of mixed optical frequency harmonics $2\omega_1 - \omega_2$ under irradiation by two monochromatic waves with the frequencies ω_1 and ω_2.

Figure 1(a) illustrates the principle of the method: two incident pump laser beams with wavelengths λ_1 (tunable from 670 nm to 980 nm) and λ_2 (1130 nm to 1450 nm) are focused collinearly onto a sample and mix together to generate a third, coherent beam of wavelength λ_e. The pump beams are generated by an optical parametric oscillator which results in collinear 6 ps pulses which overlap in time. The incident pump pulses are focused onto the sam-

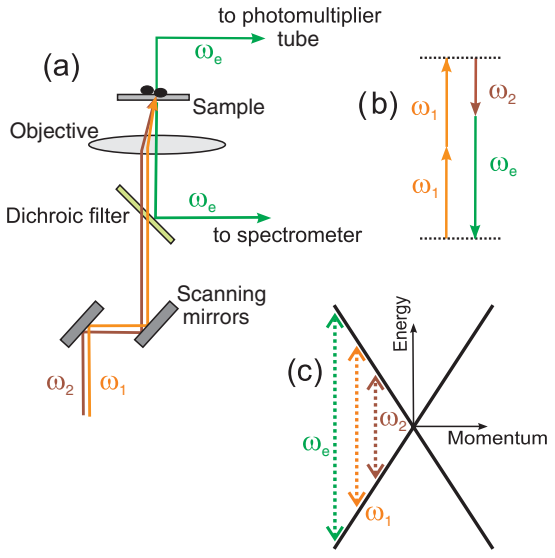

FIG. 1 (color online). (a) Schematic of the experimental layout, indicating the pump beams with frequencies ω_1, ω_2, and the emission beam with frequency ω_e. (b) Diagram of energy conservation in the four-wave mixing process. (c) Band structure of graphene with the three resonant photon energies (arrows) involved in four-wave mixing.

ple using a water immersion objective with a numerical aperture of 1.2, giving rise to a spot size <1 μm and time averaged and peak excitation powers at the sample of $\sim$1 mW and $\sim$10 W, respectively. The nonlinear emission is isolated using a 750 nm long-pass dichroic mirror followed by a 750 nm bandpass filter (210 nm bandwidth). The signal is collected in the backward direction by a spectrometer and in the forward direction by a red-sensitive photomultiplier tube (see Ref. [11] for more details of the experimental setup). Imaging is achieved by raster scanning of the excitation beams over the sample and acquiring the emitted signal as a function of its position. The wavelength range in our experiment is limited on the long-wavelength side by the filters used and at short wavelengths by the condition that $\omega_1 - \omega_2$ must be smaller than the frequency of the 2D Raman peak in graphene, in order to avoid coherent anti-Stokes Raman scattering [12].

Figure 2 shows the measured nonlinear signal from a monolayer flake as a function of emission wavelength λ_e for several combinations of pump wavelengths λ_1 and λ_2. In all measurements we observe a clear resonant spike in emission at the wavelength corresponding to the frequency $\omega_e = 2\omega_1 - \omega_2$, which indicates that the signal λ_e is generated due to coherent, third-order nonlinear optical processes (centrosymmetric materials, such as isolated sheets of graphene, do not possess second-order optical nonlinearities [13]). The amplitude of the emission peak shows a cubic dependence on the intensity of the pump pulses, which confirms the third-order nature of the response. By changing λ_1 and λ_2 we have found that, for the same pump intensities, the amplitude of the emission changes by only $\sim$10% over the used range of incident pump wavelengths.

In bulk materials the third-order nonlinearity is characterized by the third-order susceptibility $\chi^{(3)}$ which relates the polarization per unit volume P to the third power of the

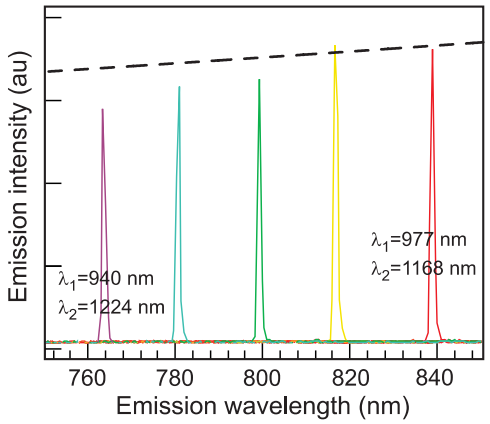

FIG. 2 (color online). Emission spectra of a graphene flake excited with pump pulses of different wavelengths, (λ_1, λ_2): (940 nm, 1224 nm), (950 nm, 1210 nm), (958 nm, 1196 nm), (967 nm, 1183 nm), and (977 nm, 1168 nm). The dashed line represents the wavelength dependence predicted by Eq. (4).

electric-field $\mathcal{E}$. In a two-dimensional conducting material like graphene it is more appropriate to describe the nonlinear response in terms of the sheet current

$$j^{(3)}(\omega_e) = \sigma^{(3)}\mathcal{E}_1(\omega_1)\mathcal{E}_2(\omega_2)\mathcal{E}_3(\omega_3), \tag{2}$$

and the third-order surface dynamical conductivity $\sigma^{(3)}$. In the degenerate four-wave mixing process used in our experiments the two mixing frequencies are equal, $\omega_1 = \omega_3$, and the frequency of emitted light is $\omega_e = 2\omega_1 - \omega_2$ due to energy conservation, Fig. 1(b).

In order to calculate the amplitude of the ω_e harmonics of the induced nonlinear current we solve the quantum kinetic equation $(i\hbar)\partial\hat{\rho}/\partial t = [\hat{H}, \hat{\rho}]$ with the Hamiltonian

$$\hat{H} = \hat{H}_0 + ex[\mathcal{E}_1 \cos\omega_1 t + \mathcal{E}_2 \cos\omega_2 t], \tag{3}$$

which describes the interaction of the electrons in graphene with electric fields of frequency ω_1 and ω_2. Here $\hat{H}_0$ is the standard tight-binding Hamiltonian of graphene, $\hat{\rho}$ is the density matrix, and x is the coordinate in the direction of the electric field. Calculating the first-order system response one gets the linear conductivity, which has been measured (with good agreement with the theory) in Ref. [7]. In the third-order in the external field amplitudes $\mathcal{E}_{1,2}$ the induced electric current $j(t)$ contains the frequency harmonics ω_1, ω_2, $3\omega_1$, $3\omega_2$, $2\omega_1 \pm \omega_2$, and $\omega_1 \pm 2\omega_2$. The component which is relevant for the experiment has the form $j^{(3)}_{\omega_e}(t) = j_e \cos(2\omega_1 - \omega_2)t$, where

$$j_e = -\frac{3}{32}\frac{e^2}{\hbar}\mathcal{E}_2\left(\frac{eV\mathcal{E}_1}{\hbar\omega_1\omega_2}\right)^2 \frac{2\omega_1^2 + 2\omega_1\omega_2 - \omega_2^2}{\omega_1(2\omega_1 - \omega_2)}. \tag{4}$$

This result is obtained under the conditions $k_B T \ll |\mu| \ll \hbar\omega_i$, $eV\mathcal{E}_{1,2}/\hbar\omega_i^2 \ll 1$, and $eV\mathcal{E}_{1,2}/|\mu|\omega_i \ll 1$, where T is the temperature and μ is the Fermi energy. Resonant enhancement of the signal due to the matching of the frequencies ω_1, ω_2 and $\omega_e = 2\omega_1 - \omega_2$ with the energies of the vertical electronic interband transitions, Fig. 1(c), is taken into account in Eq. (4). The third-order current j_e is given by the product of the linear high-frequency interband conductivity $\sim e^2/\hbar$ [5–7], the electric field $\mathcal{E}$, and the square of the electric-field parameter $\mathcal{F}_q \sim e\mathcal{E}V/\hbar\omega^2$. Here, $\mathcal{F}_q$ is the work done by the electric field during one oscillation period, $e\mathcal{E}V/\omega$, divided by the characteristic quantum energy $\hbar\omega$. [Notice that the third-order nonlinear current at low, classical frequencies ($\hbar\omega \ll |\mu|$) has a very similar structure [8], given by the product of the linear low-frequency intraband (Drude) conductivity $n_s e^2 V^2/\omega\mu$, the electric field $\mathcal{E}$ and the square of the electric-field parameter $\mathcal{F}_{\rm cl} \sim (e\mathcal{E}V/\omega\mu)$, where the energy $\hbar\omega$ is replaced by the Fermi energy μ.]

Using Eq. (4), the third-order nonlinearity of graphene can now be compared with that of other materials. This cannot be done directly, as the two-dimensional graphene is characterized by a nonlinear conductivity $\sigma^{(3)}$, while three-dimensional (bulk) materials are described by the

nonlinear susceptibility $\chi^{(3)}$. To make the comparison possible we first introduce an effective nonlinear susceptibility of graphene,

$$\chi^{(3)}_{\rm gr} \simeq \frac{\sigma^{(3)}}{\omega d_{\rm gr}}, \tag{5}$$

where $d_{\rm gr}$ is the effective thickness of a graphene layer (typically $d_{\rm gr} \simeq 3.3$ Å is normally used in the calculation of the linear optical properties of graphene [9,14–16]). Then, using $\sigma^{(3)} \simeq (e^2/\hbar)(eV/\hbar\omega^2)^2$ and the fact that the typical nonlinear susceptibility of bulk insulators is given by $\chi^{(3)}_{\rm ins} \simeq a_B^4/e^2$ [13] (a_B is the Bohr radius), we find

$$\frac{\chi^{(3)}_{\rm gr}}{\chi^{(3)}_{\rm ins}} \simeq \frac{\lambda^5}{a_B^4 d_{\rm gr}} \left(\frac{e^2}{\hbar c}\right)^3 \frac{V^2}{c^2}. \tag{6}$$

Taking $\lambda \simeq 1$ μm, $a_B \simeq d_{\rm gr} \simeq 1$ Å and using $e^2/\hbar c = 1/137$ and $V/c = 1/300$, we obtain

$$\chi^{(3)}_{\rm gr} \simeq \chi^{(3)}_{\rm ins} \times 10^8. \tag{7}$$

As insulating materials such as glasses typically exhibit $|\chi^{(3)}_{\rm ins}| \simeq 10^{-15}$ esu [13], in graphene it is expected that $|\chi^{(3)}_{\rm gr}| \simeq 10^{-7}$ esu. This considerable difference between the nonlinear response of graphene and insulating materials is due to the fact that the vertical (interband) transitions in graphene are resonant at all frequencies ω_1, ω_2 and ω_e, Fig. 1(c).

To verify this estimate of $\chi^{(3)}_{\rm gr}$ we calibrate the signal from monolayer graphene using a well-characterized, quasi-2D material: a thin film of gold ($d_{\rm Au} \simeq 4$ nm), for which the optical nonlinear susceptibility has previously been determined, $|\chi^{(3)}_{\rm Au}| \simeq 4 \times 10^{-9}$ esu [17]. Both measurements, with graphene and with the gold film, are performed under the same experimental conditions. Figure 3 shows that the gold layer exhibits a significantly smaller peak, as compared to graphene (on top of a smooth background caused by two-photon luminescence [18]). Comparing the intensities of the peaks in graphene, $I_{\rm gr}$, and in gold, $I_{\rm Au}$, with respect to the background, we find $I_{\rm gr}/I_{\rm Au} \simeq 10$. Using the relation

$$\frac{|\chi^{(3)}_{\rm gr}|}{|\chi^{(3)}_{\rm Au}|} \approx \frac{d_{\rm Au}}{d_{\rm gr}} \sqrt{\frac{I_{\rm gr}}{I_{\rm Au}}}, \tag{8}$$

and that $d_{\rm Au}/d_{\rm gr} \simeq 12$, we get the third-order susceptibility of a single graphene layer $|\chi^{(3)}_{\rm gr}| \simeq 1.5 \times 10^{-7}$ esu. Although approximate, this value agrees well with our previous estimate of 10^{-7} esu found from Eq. (7). The good agreement between experiment and theory suggests that the single electron description embodied by Eq. (4), which neglects electron-electron interactions, is adequate to describe the coherent nonlinear response of graphene.

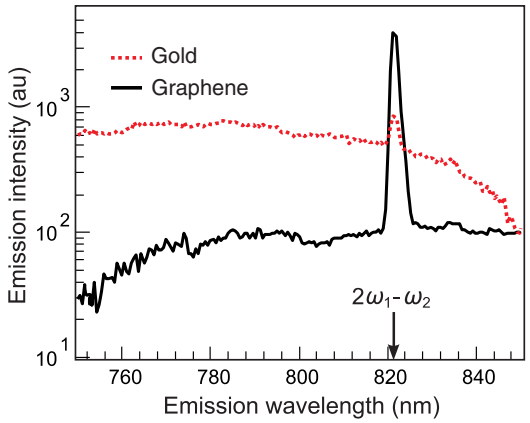

FIG. 3 (color online). Emission spectra of a graphene monolayer excited with pump wavelengths (969 nm, 1179 nm), compared to the emission of a 4 nm thick gold film under the same experimental conditions.

It is interesting to compare the nonlinear optical properties of graphene with those of semiconducting nanotubes, which also possess strong interband transitions. The nonlinear response of semiconducting carbon nanotubes is expected to be strongly dispersive, due to the singularity in electron density of states at the band edges, giving rise to sharp resonances with widths ≈1 nm [19]. In contrast, the nonlinear response of graphene given by Eq. (4) has a monotonic frequency dependence ($j_e \propto \omega^{-4}$), with a relatively weak wavelength dependence in the optical frequency range (the line in Fig. 2). This property makes graphene a particularly suitable material for broadband nonlinear applications, such as in saturable absorbers for mode-locking [20]. It is interesting to note that Eq. (4) indicates that one should expect yet stronger nonlinearities in graphene at low (far-infrared, terahertz) frequencies.

Optical microscopy is currently an important tool to find, align, and characterize graphene flakes [9,14–16]. Although it is possible to see even one atom thick graphene with optical microscopy, in practice this technique is difficult to implement due to very low imaging contrasts. The large nonlinearity in the optical properties of graphene can be utilized for a new tool for imaging and quantifying single and multilayered graphene flakes. In Fig. 4 we compare the images measured by four-wave mixing to those obtained on the same flakes by the standard optical reflection microscopy [9,15]. The striking difference in the visibility of the flakes can be quantified in terms of the image contrast, defined as

$$C = \frac{I_{\rm gr} - I_{\rm sub}}{I_{\rm sub}}, \tag{9}$$

where $I_{\rm sub}$ represents the signal from the substrate. As the dielectric substrate does not show any measurable nonlinear signal, the nonlinear contrast is very large and limited only by the noise from the detector: for a mono-

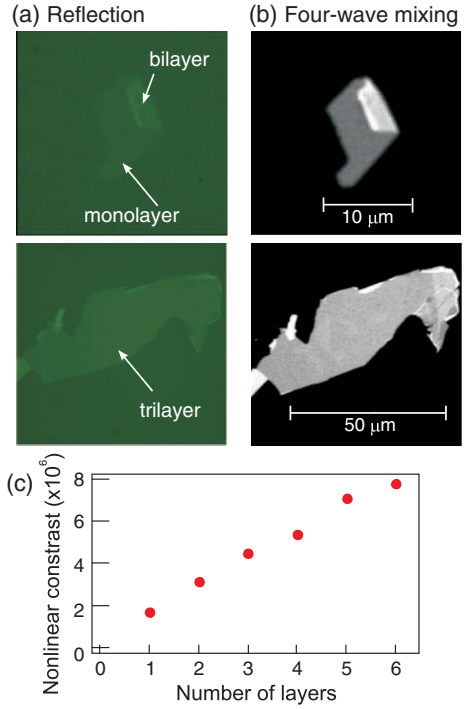

FIG. 4 (color online). (a) Standard green light (550 nm) reflection images of two graphene flakes. (b) Nonlinear optical images measured with pump wavelengths of 969 nm and 1179 nm. Image acquisition times are approximately 0.6 s. (c) The contrast in four-wave mixing images as a function of the number of graphene layers.

layer $C = 1.7 \times 10^6$ compared to $C = 0.08$ for standard optical reflection microscopy [9]. (Enhanced imaging of carbon nanotubes using nonlinear optics has been recently observed in Ref. [21].) We expect similarly high contrast for graphene on most dielectric substrates, since these materials have very weak optical nonlinearities [22].

We have also investigated the behavior of the nonlinear response of N-layered graphene flakes, Fig. 4(c). For thin graphene flakes ($N \leq 6$), the nonlinear contrast increases with N. This behavior is explained by the constructive interference of the radiated fields from different layers, as the thickness of thin flakes is significantly smaller than the wavelength of light. However, we find that thick flakes ($\gg 20$ layers) appear dark in the nonlinear images. At large N the nonlinear signal is suppressed due to two reasons. First, reflection of incident light reduces the probability of transformation of the incident frequencies of light into nonlinear harmonics. Second, the nonlinear signal generated inside a thick flake can also be reabsorbed. Solving the problem of the transmission of light through an N-layered system we obtain the expression for the intensity of the ω_e harmonics as $I_{\omega_e} \propto N^2/(1 + N\pi e^2/2\hbar c)^8$. This predicts a maximum in I_{ω_e} to occur at $N \simeq 25$.

In summary, we have performed the first measurements of the coherent nonlinear optical response of single- and few-layer graphene using four-wave mixing. Our results demonstrate that graphene exhibits a very strong nonlinear optical response in the near-infrared spectral region. The large optical nonlinearity originates from the interband electron transitions and is 8 orders of magnitude larger than the nonlinearities observed for dielectric materials without such transitions. In contrast to carbon nanotubes, the optical nonlinearity in graphene does not show resonant behavior as a function of excitation wavelength λ, but is proportional to λ^4.

This work was funded by the RCUK and EPSRC. S. A. M. acknowledges financial support from the Deutsche Forschungsgemeinschaft. The authors also wish to thank W. L. Barnes, M. Bonn, M. J. Lockyear, and A. F. Wyatt for helpful discussions.

*E.Hendry@ex.ac.uk

[1] P. R. Wallace, Phys. Rev. **71**, 622 (1947).
[2] K. S. Novoselov *et al.*, Science **306**, 666 (2004).
[3] A. K. Geim and K. S. Novoselov, Nature Mater. **6**, 183 (2007); A. K. Geim, Science **324**, 1530 (2009).
[4] A. H. C. Neto *et al.*, Rev. Mod. Phys. **81**, 109 (2009).
[5] K. F. Mak *et al.*, Phys. Rev. Lett. **101**, 196405 (2008).
[6] R. R. Nair, P. Blake, A. N. Grigorenko, K. S. Novoselov, T. J. Booth, T. Stauber, N. M. R. Peres, and A. K. Geim, Science **320**, 1308 (2008).
[7] Z. Q. Li, E. A. Henriksen, Z. Jiang, Z. Hao, M. C. Martin, P. Kim, H. L. Stormer, and D. N. Basov, Nature Phys. **4**, 532 (2008).
[8] S. A. Mikhailov, Europhys. Lett. **79**, 27002 (2007); S. A. Mikhailov and K. Ziegler, J. Phys. Condens. Matter **20**, 384204 (2008).
[9] P. E. Gaskell *et al.*, Appl. Phys. Lett. **94**, 143101 (2009).
[10] P. Ye and Y. R. Shen, Phys. Rev. A **25**, 2183 (1982).
[11] J. Moger *et al.*, Opt. Express **16**, 3408 (2008).
[12] When $\omega_1 - \omega_2$ corresponds to an optically active phonon frequency, one can observe coherent anti-Stokes Raman scattering. Since this Letter focuses on the electronic enhancement of $\chi^{(3)}$, excitation of optical phonons is avoided.
[13] R. W. Boyd, *Nonlinear Optics* (Academic Press, New York, 1992).
[14] D. S. L. Abergel, A. Russell, and Vladimir I. Fal'ko, Appl. Phys. Lett. **91**, 063125 (2007).
[15] P. Blake *et al.*, Appl. Phys. Lett. **91**, 063124 (2007).
[16] C. Casiraghi *et al.*, Nano Lett. **7**, 2711 (2007).
[17] E. Xenogiannopoulou *et al.*, Opt. Commun. **275**, 217 (2007).
[18] H. Kim *et al.*, Nano Lett. **8**, 2373 (2008).
[19] V. A. Margulis *et al.*, Opt. Commun. **249**, 339 (2005).
[20] Z. Sun *et al.*, ACS Nano **4**, 803 (2010).
[21] H. Kim *et al.*, Nano Lett. **9**, 2991 (2009).
[22] R. Adair *et al.*, J. Opt. Soc. Am. B **4**, 875 (1987).